

STRUCTURE OF INORGANIC
COMPOUNDS

Crystal Structure of Britvinite
[Pb₇(OH)₃F(BO₃)₂(CO₃)] [Mg_{4.5}(OH)₃(Si₅O₁₄)]: A New Layered
Silicate with an Original Type of Silicon–Oxygen Networks

O. V. Yakubovich^a, W. Massa^b, and N. V. Chukanov^c

^a Lomonosov Moscow State University, Leninskie gory, Moscow, 119992 Russia

e-mail: yakubol@geol.msu.ru

^b Philipps-Universität Marburg, Biegenstrasse 10, Marburg, D-35032 Germany

^c Institute of Problems of Chemical Physics, Russian Academy of Sciences, Chernogolovka, Moscow oblast, 142432 Russia

Received January 25, 2007

Abstract—The crystal structure of a new mineral britvinite Pb_{7.1}Mg_{4.5}(Si_{4.8}Al_{0.2}O₁₄)(BO₃)(CO₃)[(BO₃)_{0.7}(SiO₄)_{0.3}](OH, F)_{6.7} from the Långban iron–manganese skarn deposit (Värmland, Sweden) is determined at $T = 173$ K using X-ray diffraction (Stoe IPDS diffractometer, λ MoK α , graphite monochromator, $2\theta_{\max} = 58.43^\circ$, $R = 0.052$ for 6262 reflections). The main crystal data are as follows: $a = 9.3409(8)$ Å, $b = 9.3579(7)$ Å, $c = 18.8333(14)$ Å, $\alpha = 80.365(6)^\circ$, $\beta = 75.816 + (6)^\circ$, $\gamma = 59.870(5)^\circ$, $V = 1378.7(2)$ Å³, space group $P\bar{1}$, $Z = 2$, and $\rho_{\text{calc}} = 5.42$ g/cm³. The idealized structural formula of the mineral is represented as [Pb₇(OH)₃F(BO₃)₂(CO₃)] [Mg_{4.5}(OH)₃(Si₅O₁₄)]. It is demonstrated that the mineral britvinite is a new representative of the group of mica-like layered silicates with structures in which three-layer (2 : 1) “sandwiches” composed of tetrahedra and octahedra alternate with blocks of other compositions, such as oxide, oxide–carbonate, oxide–carbonate–sulfate, and other blocks. The tetrahedral networks (Si₅O₁₄)_∞ consisting of twelve-membered rings are fragments of the britvinite structure. Similar networks also form crystal structures of the zeophyllite mineral and the Rb₆Si₁₀O₂₃ synthetic phase. In the crystal structures under consideration, the tetrahedral networks differ in the rotation of tetrahedra with respect to the layer plane.

PACS numbers: 61.10.Nz

DOI: 10.1134/S1063774508020077

INTRODUCTION

The new mineral britvinite¹ [1] was found at the Långban iron–manganese skarn deposit (Värmland, Sweden) famed for findings of rare minerals of lead, arsenic, antimony, boron, and beryllium. Britvinite forms transparent pale yellow platelike crystals of a maximum linear size of up to 0.5 mm with a pronounced cleavage along the (001) plane in the composition of a hausmannite–barytocalcite rock, which also contains calcite, cerussite, and brucite in subordinate amounts. According to energy-dispersive X-ray microanalysis [1], the chemical composition of the mineral is as follows (wt %): PbO, 71.92; MgO, 7.95; Al₂O₃, 0.41; and SiO₂ 12.77. Moreover, it was found using selective sorption that britvinite contains 2.2%

H₂O and 2.1% CO₂. A small amount of fluorine (0.14% F) was revealed by wavelength-dispersive electron probe microanalysis. Small amounts of the compound did not allow us to determine the quantitative boron content. According to the structural data, the boron content was estimated to be 2.67% B₂O₃.

The presence of boron (revealed from the X-ray diffraction data) was confirmed by the color reaction with quinalizarin and a set of characteristic bands of (BO₃)³⁻ ions in the IR spectrum, which also involves bands associated with the stretching vibrations of OH and Si–O groups, the stretching and bending vibrations of CO₃ groups, and bending vibrations of O–Si–O groups. As follows from the IR spectroscopic data, the mineral does not contain water molecules.

The empirical formula calculated per 60 anions O + (OH,F) has the form Pb_{14.75}Mg_{9.03}Si_{9.73}Al_{0.37}O_{30.59}(BO₃)_{3.51}(CO₃)_{2.18}(OH)_{11.17}F_{0.34} ($Z = 1$). The ratio O / OH was calculated from the charge balance. The hydrogen atoms were included in

¹ The new mineral britvinite was approved by the Commission on New Minerals and Mineral Names of the Russian Mineralogical Society and the Commission on New Minerals, Nomenclature, and Classification of the International Mineralogical Association (October 17, 2006).

Table 1. Crystallographic data, experimental details, and parameters of the structure solution and refinement for the mineral britvinite $\text{Pb}_{7.1}\text{Mg}_{4.5}(\text{Si}_{4.8}\text{Al}_{0.2}\text{O}_{14})(\text{BO}_3)(\text{CO}_3)[(\text{BO}_3)_{0.7}(\text{SiO}_4)_{0.3}](\text{OH})_{5.7}\text{F}$

Absorption coefficient μ , mm^{-1}	43.71
Space group, Z	$P\bar{1}$, 2
Unit cell parameters (\AA) and angles (deg)	
<i>a</i>	9.3409(8)
<i>b</i>	9.3579(7)
<i>c</i>	18.8333(14)
α	80.365(6)
β	75.816(6)
γ	59.870(5)
Unit cell volume V , \AA^3	1378.7(2)
Density ρ_{calcd} , g/cm^3	5.42
Diffractometer	IPDS-II area detector system (Stoe)
Radiation	$\text{MoK}\alpha$ (graphite monochromator)
Temperature, K	173(2)
Scan range: $2\theta_{\text{max}}$, deg	58.43
Number of reflections measured	18335
Number of unique reflections/number of reflections with $I > 1.96\sigma(I)$	7381/6262
Refinement technique	on F^2
Number of parameters refined	547
Absorption correction	Empirical
T_{min} , T_{max}	0.022; 0.212
R_{int} , R_{σ}	0.070; 0.057
Secondary extinction coefficient	0.0015(1)
Discrepancy factors:	
<i>R</i> (for reflections observed)	0.0517
wR^2 (for all unique reflections)	0.1250
<i>s</i>	1.129
Residual electron density, ρ_{max} , ρ_{min} , e \AA^{-3}	4.09 (0.78 \AA for Pb5) -2.92 (0.82 \AA for Pb3)

the composition of OH groups according to the IR spectroscopic data.

X-RAY DIFFRACTION ANALYSIS AND REFINEMENT OF THE STRUCTURE

The unit cell parameters and triclinic symmetry were revealed in the X-ray diffraction study of a plate-like single-crystal grain $0.12 \times 0.08 \times 0.04$ mm in size on a Stoe diffractometer ($\text{MoK}\alpha$ radiation, graphite monochromator) equipped with a high-sensitivity imaging plate detector [2]. The reflection intensities measured on the same diffractometer at $T = 173$ K were corrected for the Lorentz and polarization factors. The empirical absorption correction accounting for the size and shape of the sample was also applied to the reflection intensities. The crystallographic data, experimental

details, and parameters of the structure solution and refinement for the britvinite are summarized in Table 1.

All the calculations associated with the solution and refinement of the structure were performed with the SHELX software package [3, 4]. The atomic scattering factors and corrections for anomalous dispersion were taken from [5]. The structure was refined in space group $P\bar{1}$ on F^2 to $R = 0.0517$ [for 6262 reflections with $I \geq 2\sigma(I)$] in the anisotropic approximation for the majority of the atoms involved. The coordinates of the basis atoms and thermal parameters are listed in Table 2.²

ANALYSIS OF THE INTERATOMIC DISTANCES

In the crystal structure of the britvinite, five crystallographically independent manganese atoms have an

² Additional information can be found in database no. 418 545.

Table 2. Coordinates of the basis atoms and equivalent thermal parameters

Atom	x/a	y/b	z/c	U_{eq}	Site occupancy
Si(1)	0.6638(4)	0.6431(4)	0.34874(17)	0.0149(6)	1
Si(2)	0.3603(4)	0.2950(4)	0.34902(17)	0.0142(6)	1
Si(3)	0.6753(4)	0.9600(4)	0.35497(17)	0.0147(6)	1
Si(4)	0.3423(4)	0.6272(4)	0.35457(16)	0.0135(6)	1
Si(5)	0.0107(4)	0.9466(4)	0.34929(16)	0.0132(6)	1
Mg(1)	0.5	0.5	0.5	0.0136(10)	1
Mg(2)	0.8369(5)	0.1664(4)	0.4964(2)	0.0134(7)	1
Mg(3)	0.1671(5)	0.1689(4)	0.4959(2)	0.0131(7)	1
Mg(4)	0.8354(5)	0.4987(4)	0.4971(2)	0.0128(7)	1
Mg(5)	0.4993(5)	0.8330(4)	0.5000(2)	0.0134(7)	1
Pb(1)	0.06509(6)	0.53207(6)	0.23857(3)	0.02045(17)	0.952(6)
Pb(1A)	0.173(4)	0.653(3)	0.234(1)	0.032(3)*	0.020(2)
Pb(1B)	0.973(6)	0.719(6)	0.236(3)	0.032(3)*	0.012(2)
Pb(2)	0.28960(6)	0.07376(5)	0.23590(3)	0.01878(17)	0.961(6)
Pb(2A)	0.406(4)	0.875(3)	0.235(1)	0.032(3)*	0.020(2)
Pb(2B)	0.502(6)	0.973(6)	0.238(2)	0.032(3)*	0.012(2)
Pb(3)	0.82941(6)	0.30837(5)	0.23655(3)	0.01878(17)	0.958(6)
Pb(3A)	0.744(5)	0.191(4)	0.240(2)	0.032(3)*	0.016(2)
Pb(3B)	0.631(5)	0.409(5)	0.241(2)	0.032(3)*	0.014(2)
Pb(4)	0.77275(8)	0.97209(7)	0.14948(3)	0.0299(2)	0.964(6)
Pb(5)	0.4359(6)	0.6395(9)	0.1480(3)	0.0279(7)	0.60(5)
Pb(5A)	0.4405(10)	0.6609(19)	0.1383(10)	0.0341(18)	0.35(5)
Pb(6)	0.836(2)	0.2432(11)	0.9967(4)	0.0463(16)	0.44(2)
Pb(6A)	0.9190(5)	0.2396(4)	0.0138(2)	0.0318(13)	0.202(5)
Pb(6B)	0.785(2)	0.280(3)	0.0043(7)	0.042(4)	0.26(2)
Pb(6C)	0.7228(17)	0.379(3)	0.0015(7)	0.032(3)	0.053(5)
Pb(7)	0.1188(8)	0.3166(8)	0.0776(1)	0.0521(13)	0.433(15)
Pb(7A)	0.1397(3)	0.3622(8)	0.0772(1)	0.0237(11)	0.346(15)
Pb(8)	0.5716(4)	0.0521(7)	0.9995(1)	0.0302(10)	0.283(6)
Pb(8A)	0.6098(5)	0.9712(9)	0.9857(2)	0.0248(15)	0.176(6)
C(1)	0.783(2)	0.6505(18)	0.1168(8)	0.028(3)	1
B(1)	0.1071(19)	0.9784(18)	0.1280(8)	0.022(3)	1
B(2)	0.447(2)	0.315(2)	0.1284(9)	0.013(2)*	0.734(11)
Si(6)	0.4644(15)	0.3212(14)	0.0808(6)	0.013(2)*	0.266(11)
O(1)	0.6361(10)	0.6207(9)	0.4378(4)	0.0151(15)	1
O(2)	0.4502(19)	0.6770(18)	0.0277(6)	0.046(3)	1
O(3)	0.2322(12)	0.2934(11)	0.3054(5)	0.0211(17)	1
O(4)	0.0331(10)	0.3816(10)	0.5564(4)	0.0156(15)	1
O(5)	0.9680(10)	0.2829(9)	0.4432(4)	0.0132(14)	1
O(6)	0.3665(11)	0.7153(10)	0.5560(4)	0.0154(15)	1
O(7)	0.9717(10)	0.9504(10)	0.4385(4)	0.0151(15)	1
O(8)	0.3071(10)	0.2874(9)	0.4375(4)	0.0140(14)	1
O(9)	0.8351(11)	0.5024(11)	0.3064(5)	0.0221(17)	1
O(10)	0.7005(10)	0.0494(9)	0.5553(4)	0.0149(14)	1

Table 2. (Contd.)

Atom	<i>x/a</i>	<i>y/b</i>	<i>z/c</i>	<i>U</i> _{eq}	Site occupancy
O(11)	0.6361(10)	0.9507(10)	0.4430(4)	0.0148(15)	1
O(12)	0.3047(10)	0.6156(9)	0.4422(4)	0.0135(14)	1
O(13)	0.3748(13)	0.4629(11)	0.3202(4)	0.0219(17)	1
O(14)	0.8677(12)	0.9271(12)	0.3216(5)	0.0233(18)	1
O(15)	0.5075(12)	0.6496(12)	0.3310(5)	0.0214(17)	1
O(16)	0.5487(12)	0.1418(10)	0.3226(5)	0.0204(17)	1
O(17)	0.1873(11)	0.7824(12)	0.3220(5)	0.0223(17)	1
O(18)	0.9177(15)	0.6512(14)	0.1166(6)	0.034(2)	1
O(19)	0.0212(12)	0.1055(11)	0.3048(5)	0.0231(18)	1
O(20)	0.7507(14)	0.0182(15)	0.8746(7)	0.036(2)	1
O(21)	0.8245(15)	0.0065(13)	0.0289(5)	0.030(2)	1
O(22)	0.6533(11)	0.8235(11)	0.3222(5)	0.0197(16)	1
O(23)	0.8937(13)	0.1607(12)	0.8732(5)	0.028(2)	1
O(24)	0.7797(15)	0.5148(14)	0.1155(7)	0.035(2)	1
O(25)	0.6452(16)	0.7867(14)	0.1218(6)	0.037(2)	1
O(26)	0.3023(17)	0.4579(15)	0.1222(7)	0.045(3)	1
O(27)	0.5825(15)	0.3152(16)	0.1299(6)	0.039(3)	1
O(28)	0.4502(15)	0.1720(13)	0.1273(6)	0.035(2)	1
O(29)	0.9599(13)	0.1223(14)	0.1307(6)	0.034(2)	1
F(1)	0.0789(11)	0.3118(10)	0.1942(5)	0.0107(15)*	0.719(14)
F(1 <i>a</i>)	0.101(3)	0.317(2)	0.1472(12)	0.0107(15)*	0.281(14)

* Thermal parameters of the atoms refined in the isotropic approximation. The thermal parameters of the Pb(1A), Pb(1B), Pb(2A), Pb(2B), Pb(3A), and Pb(3B) atoms were refined using the same value. The pairs of the atoms B(2), Si(6) and F(1), F(1*a*) were refined similarly.

octahedral environment of oxygen atoms. In the centrosymmetric octahedra of the Mg(1) atoms, the Mg–O interatomic bonds vary from 2.066(8) to 2.128(8) Å (the mean distance, 2.088 Å). The Mg–O bond lengths in the other polyhedra around the magnesium atoms in the general position have a larger spread and lie in the range 2.019(8)–2.158(8) Å. The mean values of the Mg–O distances in five independent octahedra are close in magnitude and equal to 2.09 Å to the second decimal place.

The Si–O bond lengths in five independent Si tetrahedra range from 1.593(9) to 1.644(9) Å. A strong distortion of the tetrahedra is due to their interaction with each other through common oxygen atoms: either of the two tetrahedra has three common vertices with the neighboring tetrahedra, and three tetrahedra each have two common vertices. A small number of Al atoms revealed in the crystal composition by electron probe microanalysis reflect on the mean distances of the Si–O bonds: Si(1)–O, 1.625 Å; Si(2)–O, 1.626 Å; Si(3)–O, 1.624 Å; Si(4)–O, 1.613 Å; and Si(5)–O, 1.631 Å. Probably, the Si(4) polyhedra do not contain Al atoms. Most likely, the Al atoms isomorphously occupy the other tetrahedra, so that the maximum occupation of aluminum is observed for the Si(5) tetrahedron.

The carbon and boron atoms form planar trigonal oxo complexes. In the nearly regular triangles CO₃, the C–O bond lengths vary from 1.26(2) to 1.28(2) Å (the mean distance, 1.27 Å). The B–O distances in the trigonal groups around the B(1) and B(2) atoms are naturally larger and lie in the ranges 1.31(2)–1.36(2) and 1.27(2)–1.35(2) Å, respectively. The cation–oxygen distances in the boron triangles indicate that, possibly, the B(1) and B(2) atoms are “diluted” by carbon atoms with a smaller size. The oxygen triangle around the B(2) atom can be interpreted as a face occupied by the boron atom in the Si(6) tetrahedron (Fig. 1). The interatomic distance B(2)–Si(6) equal to 0.87 Å excludes the simultaneous occupation of the corresponding structural positions by the B and Si atoms. The refinement of the occupancies revealed that these positions are statistically occupied in the ratio 0.74[B(2)] : 0.26[Si(6)]. A considerable spread in the interatomic distances in the Si(6) tetrahedron manifests itself in shortened lengths of the Si–O bonds to the oxygen atoms that form the trigonal face occupied by the boron atom with a probability of 74% in the tetrahedron and, conversely, in a too long bond to the O(2) atom is associated with the tendency toward a displacement of the Si(6) atom from the Pb(6) and Pb(7) cations (Fig. 1). It

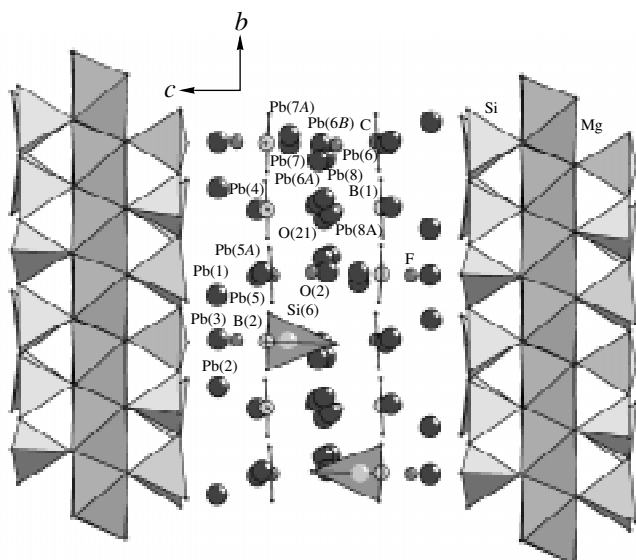


Fig. 1. Three-layer pyrophyllite sandwiches and $[\text{Pb}_{7.1}(\text{OH})_{2.7}\text{F}(\text{CO}_3)(\text{BO}_3)_{1.7}(\text{SiO}_4)_{0.3}]_{\infty}$ five-layer stacks alternating along the c axis in the unit cell of the crystal structure of britvinite.

should be noted that an unusual distortion of silicon tetrahedra is also described, for example, in the structure of sakhaite [6]. Furthermore, boron tetrahedra with bond lengths that differ substantially from conventional bond lengths are well known in the structures of cubic boracite and its numerous synthetic varieties [7].

The Pb–O interatomic distances for all the located lead atoms are similar to conventional distances and lie in the range 2.20(1)–3.03(1) Å. The Pb–F distances are somewhat shorter and can be as small as 2.14(1) Å. The mean lengths of the Pb–O(F) bonds vary from 2.46 to 2.75 Å. The O^{2-} and F^- anions forming the polyhedra around the Pb atoms are located, as is frequently the case, on one side of the Pb^{2+} cation (an umbrella configuration) and, thus, fix the position of a lone electron pair.

DESCRIPTION OF THE CRYSTAL STRUCTURE

Two types of blocks that alternate along the c axis in the triclinic unit cell form the crystal structure of the britvinite (Fig. 1). Blocks of the first type are formed by brucite-like layers composed of edge-shared Mg octahedra bounded on both sides along the c axis by networks of silicon–oxygen tetrahedra. The apical vertices of the tetrahedra are directed toward the close-packed octahedral layers, and the blocks under consideration can be interpreted as three-layer sandwiches of the composition $\{\text{Mg}_{4.5}(\text{OH})_3[(\text{Si}, \text{Al})_5\text{O}_{14}]\}_{\infty}$. The networks of vertex-shared tetrahedra (Fig. 2) are similar to tetrahedral layers in micas: if each central tetrahedron joining three neighboring six-membered rings in the tetrahedral layer is removed from the crystal structure

of mica, there appear $(\text{Si}_5\text{O}_{14})_{\infty}^{8-}$ networks of the new type revealed in the structure of britvinite.

Blocks of the second type are seven-layer stacks that are parallel to the ab plane, consist of Pb^{2+} cations, which are partially coordinated by oxygen atoms of hydroxyl groups and fluorine atoms, and planar trigonal groups CO_3 and BO_3 , and are described by the formula $[\text{Pb}_{7.1}(\text{OH})_{2.7}\text{F}(\text{CO}_3)(\text{BO}_3)_{1.7}(\text{SiO}_4)_{0.3}]_{\infty}$. In the layer, the CO_3 and BO_3 trigonal groups alternate in a ratio of $\sim 2 : 1$ along the b axis and their planes are parallel to the (001) plane (Fig. 1).

The specific feature of this structural component of britvinite is its defect structure. Among eight independent lead atoms involved in the formation of the crystal structure of the mineral, the positions of four atoms Pb(5)–Pb(8) are split into two or three positions with comparable occupancies. Moreover, the Pb(7) and Pb(8) positions contain a large number of vacancies (Table 2). The presence of additional weakly occupied Pb positions at distances of ~ 1.2 – 1.8 Å from the positions of the “main” atoms Pb(1), Pb(2), and Pb(3) with a high occupancy in the same planes as the main atoms correlates with the observed diffuse bands along the c^* direction of the reciprocal lattice (Fig. 3). The diffuse scattering from lead atoms is associated with the one-dimensional disorder. The translational silicon–oxygen layers, which form the structure of britvinite, are parallel to the ab plane, and contain ordered vacancies, are displaced with respect to the layers composed of the Pb(1), Pb(2), and Pb(3) atoms, so that the “vacant” tetrahedra and, hence, the Pb atoms appear to be displaced in the second and third equivalent layers (Fig. 2). As a result, the additional lead atoms Pb(1A), Pb(1B), Pb(2A), Pb(2B), Pb(3A), and Pb(3B) (stacking disorder) manifest themselves in the diffraction experiment.

In the framework of the proposed model, the layer that is composed of the Pb(1), Pb(2), and Pb(3) atoms and located in the vicinity of the silicon–oxygen networks (the “first” layer) does not contain defects. The presence of the additional lead atoms Pb(1A), Pb(1B), Pb(2A), Pb(2B), Pb(3A), and Pb(3B) is associated with the stacking faults in the equivalent silicon–oxygen networks and lead layers contacting with the networks through common oxygen atoms (Fig. 2). The other five layers composed of Pb atoms (with additional atoms B and C) do not have direct contacts with “pyrophyllite” sandwiches, and, in this case, all cations are coordinated by “own” atoms O and F. The majority of the Pb atoms forming these layers are statistically disordered but also lie within the ab planes. The first lead layer is most likely responsible for the joining of the ordered pyrophyllite block $\{\text{Mg}_{4.5}(\text{OH})_3[(\text{Si}, \text{Al})_5\text{O}_{14}]\}_{\infty}$ and the defect block $[\text{Pb}_{7.1}(\text{OH})_{2.7}\text{F}(\text{CO}_3)(\text{BO}_3)_{1.7}(\text{SiO}_4)_{0.3}]_{\infty}$ into the single crystal structure of britvinite.

Blocks of the second type can be treated as an association of modified layers of the structure of synthetic

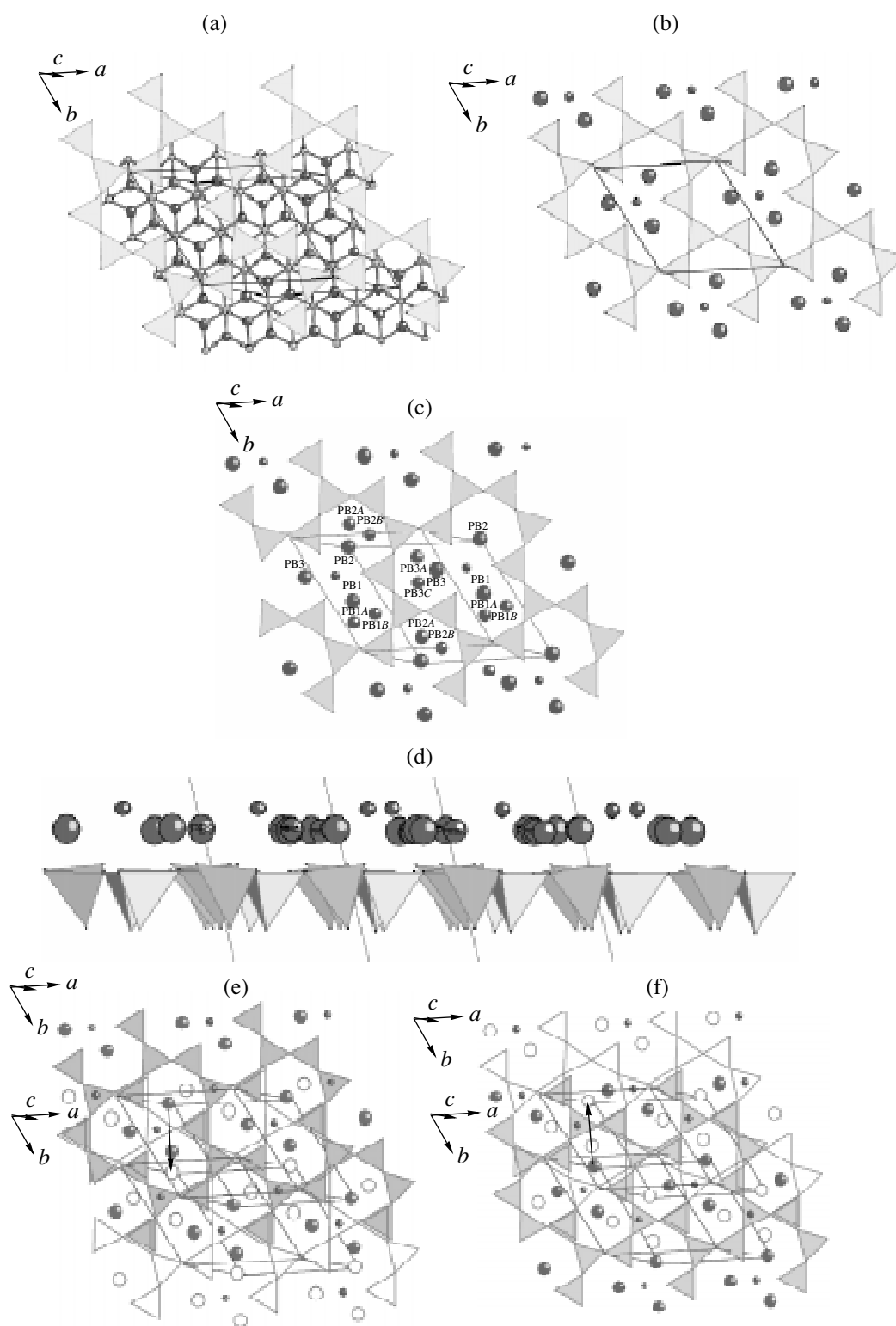


Fig. 2. (a) Brucite layer composed of Mg octahedra and the adjacent silicon–oxygen network consisting of twelve-membered rings in the crystal structure of britvinite (the view along the c axis of the unit cell). (b) Silicon–oxygen network and the first layer of the Pb block (theoretical representation). (c) Silicon–oxygen network and the first layer of the Pb block according to the results of the structure refinement. Large spheres indicate the positions of the Pb atoms with a high occupancy, medium spheres represent the positions of the Pb atoms with a low occupancy, and small spheres correspond to the F atoms. (d) The same fragment but viewed from the side. (e) Superposition of the first and second equivalent fragments displaced with respect to each other (along the arrow). (f) Superposition of the first and third equivalent fragments displaced with respect to each other (along the arrow).

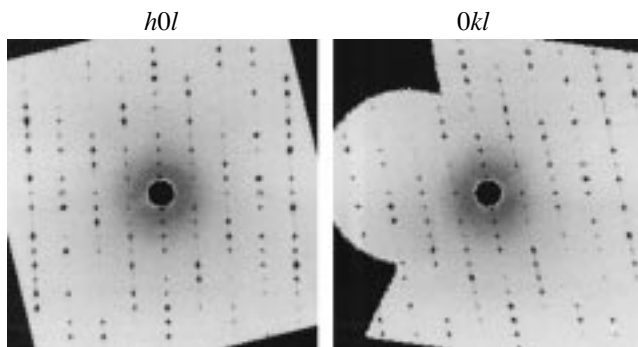


Fig. 3. Diffuse lines along the c^* direction of the reciprocal lattice of britvinite.

plumbonacrite $\text{Pb}_5\text{O}(\text{OH})_2(\text{CO}_3)_3$ [8] with partially split Pb positions and one-third of carbonate groups replaced by borate triangles. According to Krivovichev and Burns [8], plumbonacrite easily transforms into hydrocerussite $2(\text{PbCO}_3)\text{Pb}(\text{OH})_2$, which has a similar structure that consists of alternating lead carbonate and lead hydroxide layers. Layers of the same composition form the crystal structures of trimorphic minerals, such as leadhillite [9], macphersonite [10], and susannite [11] $\text{Pb}_4(\text{CO}_3)_2(\text{OH})_2(\text{SO}_4)$; however, these structures additionally contain layers of orthosulfate tetrahedra. The alternation of similar layers in these structures can be written as follows: $\dots\text{SO}_4\text{-Pb}(\text{OH})_2\text{-Pb}(\text{CO}_3)\text{-Pb}(\text{CO}_3)\text{-Pb}(\text{OH})_2\text{-SO}_4\text{-}\dots$

COMPARISON OF THE CRYSTAL STRUCTURE OF BRITVINITE WITH THE STRUCTURES OF THE RELATED PHASES

The results obtained allow us to argue that the britvinite is a new representative of the group of mica-like mixed layered silicates with structures in which three-layer (2 : 1) sandwiches composed of tetrahedra and octahedra alternate with blocks of other compositions, such as oxide, oxide-carbonate, oxide-carbonate-sulfate, and other blocks. This group involves the minerals macaulayite, lourenswalsite, burckhardtite, kegelite, surite, ferrisurite [12], and niksergievite [13] (Table 3). In the absence of data of precision X-ray structure investigations, the preliminary inferences regarding their structure were made using the results of chemical spectroscopic, and X-ray powder diffraction analyses and, in a number of cases, microdiffraction experiments.

In particular, the crystal structure of surite $[(\text{PbCO}_3)_2(\text{Ca}_{0.5}\text{OH})][(\text{Al}, \text{Mg})_2(\text{OH})_2(\text{Si}, \text{Al})_4\text{O}_{10}]$ [14] is considered a mixed layered phase formed by alternating blocks, i.e., structural fragments of pyrophyllite (where Al in octahedra and Si in tetrahedra are partially replaced by Mg and Al, respectively) and hydrocerussite modified by partial substitution of calcium for lead. In isostructural ferrisurite [15], the gibbsite octahedral layer of the "ferripyrophyllite stack" is probably occu-

ried by Fe^{3+} and Al cations in accordance with the hypothetical crystal chemical formula of the mineral $[(\text{Pb}, \text{Ca})_{2-3}(\text{CO}_3)_{1.5-2}(\text{OH}, \text{F})_{0.5-1}n\text{H}_2\text{O}][(\text{Fe}, \text{Al})_2(\text{OH})_2\text{Si}_4\text{O}_{10}]$. In the structure of kegelite $[\text{Pb}_4(\text{CO}_3)_2(\text{OH})_2(\text{SO}_4)][\text{Al}_2(\text{OH})_2\text{Si}_4\text{O}_{10}]$ [16], the pyrophyllite stacks most likely alternate with the blocks of monoclinic leadhillite along the c axis. In the crystal structure of macaulayite [17], the ferripyrophyllite fragments probably alternate with the hematite blocks:

$[(\text{Fe}_2\text{O}_3)_{11}][\text{Fe}_2^{3+}(\text{OH})_2\text{Si}_4\text{O}_{10}]$. In the structure of burckhardtite [18], the positions in gibbsite octahedra can be treated as occupied by Fe^{3+} and Te^{4+} cations (the octahedral environment consisting of oxygen atoms is typical of Te^{4+} ions, as is the case in the structures of the jensenite, leisingite, and parakhinite minerals) with the formation of neutral stacks of the pyrophyllite structure, between which the lead oxide hydroxide lamellas are incorporated: $[\text{PbO} \cdot \text{Pb}(\text{OH})_2][\text{FeTe}(\text{OH})_2(\text{AlSi}_3\text{O}_{10})]$. In the crystal structure of niksergievite [13], the three-layer sandwiches, i.e., the fragments of dioctahedral Al mica $[\text{Al}_2(\text{OH})_2\text{AlSi}_3\text{O}_{10}]_{\infty}$, alternate with the multilayer stacks of the complex composition $[(\text{Ba}, \text{Ca})_2\text{Al}(\text{OH})_4(\text{CO}_3) \cdot n\text{H}_2\text{O}]_{\infty}$. The crystal structure of the last mineral of the group under consideration, namely, hexagonal lourenswalsite [19], possibly contains the three-layer blocks $[(\text{Ti}^{4+}\text{Fe}_{0.5}^{3+})\text{O}_3(\text{Si}_4\text{AlO}_{14})]_{\infty}$, which are topologically similar to the mica-like blocks in the crystal structure of britvinite but have a different chemical composition. These blocks along the c axis alternate with the fragments of the composition $[(\text{K}, \text{Ba})_2(\text{OH})_5 \cdot 4\text{H}_2\text{O}]_{\infty}$.

The mineral group under investigation can be interpreted in the framework of the modular concept under the assumption that the pyrophyllite (mica) three-layer sandwich composed of octahedra and tetrahedra is an extreme member of the polysomatic series. In the strict sense, the sandwiches under consideration are not identical in the structures of different representatives of the given mineral group. The anion sublattice consisting of oxygen atoms is the same in all crystal structures; however, the occupation octahedral and tetrahedral holes is most likely different in character. Reasoning from the hypothetical crystal chemical formulas of the minerals, we can make the inference that the central octahedral layers in the three-layer sandwiches can be brucite or gibbsite (as in the structures of micas) and the tetrahedral "chain armor" can differ in the number of occupied tetrahedra in the network. As was shown above, the pyrophyllite three-layer sandwiches along the c axis of the unit cells of the structures of this series alternate with multilayer lamellar stacks that have different compositions and structures.

Tetrahedral networks $(\text{Si}_5\text{O}_{14})_{\infty}$ (consisting of twelve-membered rings) similar to those in the structure of britvinite are described in the structure of zeophyllite (calcium silicate mineral) $\text{Ca}_{13}(\text{F}, \text{OH})_{10}[\text{Si}_5\text{O}_{14}]_2 \cdot 6\text{H}_2\text{O}$

Table 3. Selected crystal chemical and crystallographic data for complex mica-like silicates with structures of the modular type (the macaulayite–burckhardtite group [12])

Mineral	Formula of the silicate stack	Formula of the block of variable composition	Unit cell parameters ($a, b, c, \text{\AA}$) and angles ($\alpha, \beta, \gamma, \text{deg}$)	Unit cell volume, (\AA^3)	Symmetry, space group (possible)	Z	Density ρ_{calcd} , g/cm ³	References
Britvinite	$\text{Mg}_{4.5}(\text{OH})_3(\text{Si}_5\text{O}_{14})$	$\text{Pb}_7(\text{OH})_3\text{F}(\text{BO}_3)_2(\text{CO}_3)$	$a = 9.3409(8)$ $\alpha = 80.365(6)$ $b = 9.3597(7)$ $\beta = 75.816(6)$ $c = 18.833(1)$ $\gamma = 59.870(5)$	1378.7	Triclinic $P\bar{1}$	2	5.42	This study
Surite	$(\text{Al, Mg})_2(\text{OH})_2(\text{Si, Al})_4\text{O}_{10}$	$(\text{PbCO}_3)_2(\text{Ca}_{0.5}\text{OH})$	$a = 5.219(2)$ $b = 8.968(2)$ $\beta = 90.13(5)$ $c = 16.190(2)$	757.8	Monoclinic $P2_1/m, P2_1$	2	4.00	14
Ferrisurite	$(\text{Fe, Al})_2(\text{OH})_2\text{Si}_4\text{O}_{10}$	$(\text{Pb, Ca})_{2-3}(\text{CO}_3)_{1.5-2}(\text{OH, F})_{0.5-1}n\text{H}_2\text{O}$	$a = 5.241(1)$ $b = 9.076(5)$ $\beta = 90.03(7)$ $c = 16.23(1)$	772	Monoclinic $P2_1/m, P2_1$	2	3.89	15
Kegelite	$\text{Al}_2(\text{OH})_2\text{Si}_4\text{O}_{10}$	$\text{Pb}_4(\text{CO}_3)_2(\text{OH})_2(\text{SO}_4)$	$a = 8.986(6)$ $b = 15.55(1)$ $\beta = 91.0(1)$ $c = 21.04(1)$	2939.5	Monoclinic $C2/m, C2, Cm$	6	4.76	16
Macaulayite	$\text{Fe}_2^{3+}(\text{OH})_2\text{Si}_4\text{O}_{10}$	$(\text{Fe}_2\text{O}_3)_{11}$	$a = 5.038$ $b = 8.726$ $\beta = 92$ $c = 36.342$	1596.0	Monoclinic Bravais lattice C	6	4.41	17
Burckhardtite	$\text{FeTe}(\text{OH})_2(\text{AlSi}_3\text{O}_{10})$	$\text{PbO} \cdot \text{Pb}(\text{OH})_2$	$a = 5.21$ $b = 9.04$ $\beta = 90$ $c = 12.85$	629.3	Monoclinic Bravais lattice C	2	4.96	18
Niksergievite	$\text{Al}_2(\text{OH})_2\text{AlSi}_3\text{O}_{10}$	$(\text{Ba, Ca})_2\text{Al}(\text{OH})_4(\text{CO}_3) \cdot n\text{H}_2\text{O}$	$a = 5.176$ $\beta = 96.44$ $b = 8.989$ $c = 16.166$	747.4	Monoclinic $C2/m, C2, Cm$	2	3.21	13
Lourenswalsite	$(\text{Ti}_4^{4+} \text{Fe}_{0.5}^{3+})\text{O}_3(\text{Si}_4\text{AlO}_{14})$	$(\text{K, Ba})_2(\text{OH})_5 \cdot 4\text{H}_2\text{O}$	$a = 5.244(2)$ $c = 20.49(3)$	488.0	Hexagonal	1	3.20	19

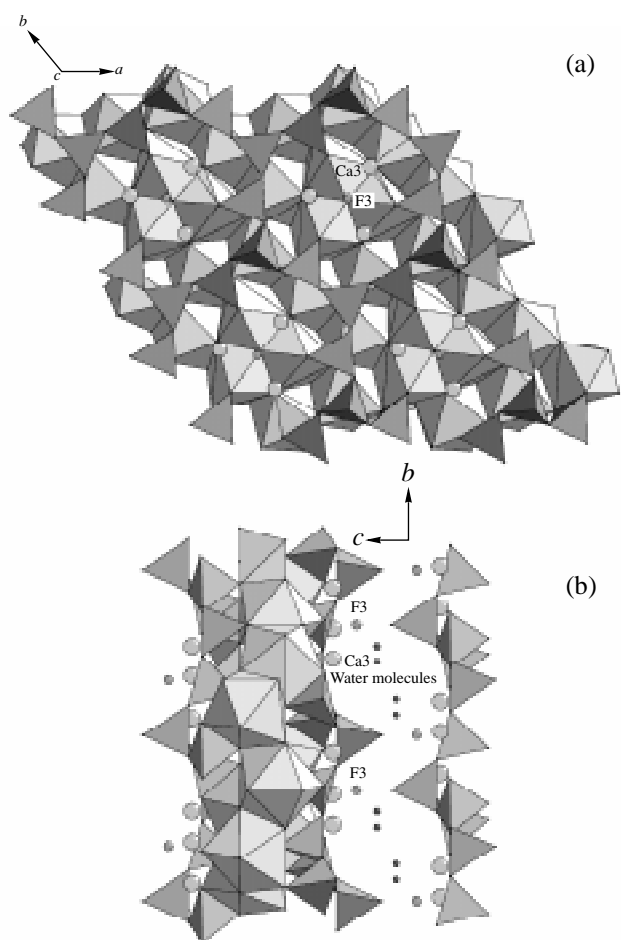


Fig. 4. Crystal structure of zeophyllite: (a) projection onto the ab plane and (b) fragment of the crystal structure in the projection onto the bc plane.

[20, 21]. The same formula of the two-dimensional silicon–oxygen radical describes tetrahedral networks topologically similar in the (001) plane; however, the orientation of silicon tetrahedra with respect to the network planes in the structures of these minerals is different: the apical vertices of all tetrahedra in the structure of britvinite are directed to the same side ($UUU\dots$), whereas each fourth tetrahedron in the structure of zeophyllite is rotated in the opposite direction ($UUUDUUUD\dots$) (Fig. 4). The rotation of a number of tetrahedra with respect to the network plane in the structure of zeophyllite as compared to the structure of britvinite is a direct consequence of the occupation of the central layer (between two tetrahedral networks) by Ca^{2+} cations that are larger than Mg^{2+} cations. This rotation is necessary for ensuring a correspondence between the two-dimensional silicon–oxygen radical anion $(\text{Si}_5\text{O}_{14})_{\infty}$ and the wavy close-packed layer composed of octahedra and Ca eight-vertex polyhedra. The structure of three-layer sandwiches in the crystal structures of britvinite $\{\text{Mg}_{4.5}(\text{OH})_3[(\text{Si}, \text{Al})_5\text{O}_{14}]\}_{\infty}$ and zeophyllite $\{\text{Ca}_{3.5}(\text{F},$

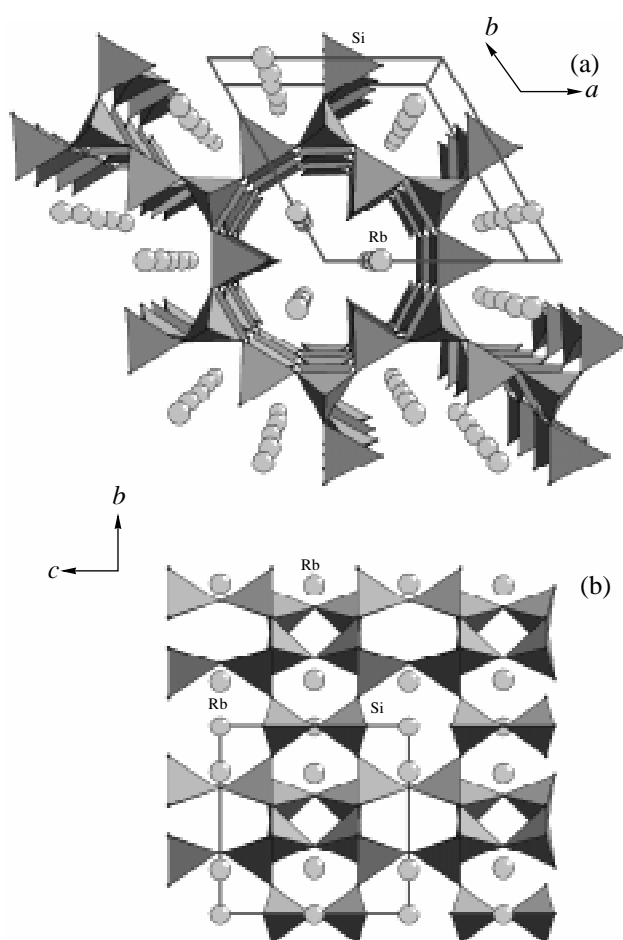


Fig. 5. Three-dimensional tetrahedral framework of the crystal structure of the $\text{Rb}_6\text{Si}_{10}\text{O}_{23}$ compound: (a) view along the c axis and (b) projection onto the bc plane.

$\text{OH})_4(\text{Si}_5\text{O}_{14})_{\infty}$ is a good example illustrating that the “flexibility” of tetrahedral silicon–oxygen radical anions allow them to be “adopted” to the cation component of the structure [22].

The crystal structures of the hexagonal and orthorhombic modifications of the synthetic compound $\text{Rb}_6\text{Si}_{10}\text{O}_{23}$ are based on the three-dimensional tetrahedral framework described by the formula $(\text{Si}_{10}\text{O}_{23})_{\infty}$ [23]. The three-dimensional silicate paraframework is formed by condensation of networks of the composition $(\text{Si}_{10}\text{O}_{28})_{\infty} = 2(\text{Si}_5\text{O}_{14})_{\infty}$ that, in the (001) plane, are topologically identical to the silicon–oxygen layers in the crystal structures of britvinite and zeophyllite. The twelve-membered rings composed of Si tetrahedra shared by the oxygen vertices form two-dimensional network layers, as is the case in the structures of britvinite and zeophyllite. However, the rotations of the tetrahedra with respect to the plane of these layers are different. In particular, in the framework crystal structures of the low-temperature orthorhombic and high-temperature hexagonal modifications of the $\text{Rb}_6\text{Si}_{10}\text{O}_{23}$ com-

pound, the apical oxygen vertices of the tetrahedra neighboring in the (001) plane are alternately directed upward and downward with respect to the layer plane (UDUDUD...) (Fig. 5). The neighboring silicon-oxygen layers are joined together by the same oxygen vertices of the tetrahedra into a framework that have wide channels composed of twelve-membered rings and extended along the *c* axis and six-membered windows open in the perpendicular directions.

ACKNOWLEDGMENTS

1 We would like to thank I.A. Bryzgalov for examining the crystals on the wavelength-dispersive electron probe microanalyzer.

This study was supported by the Russian Foundation for Basic Research (project no. 05-05-64721) and the Deutsche Akademie der Wissenschaften.

REFERENCES

1. N. V. Chukanov, O. V. Yakubovich, I. V. Pekov, et al., *Zap. Vseross. Mineral. O-va.* (in press).
2. *STOE and Cie: Imaging Plate Diffraction System (IPDS), Version 2.90* (STOE and Cie, Darmstadt, Germany, 1999).
3. G. M. Sheldrick, *SHELXS97: Program for the Solution of Crystal Structures* (University of Göttingen, Göttingen, Germany, 1997).
4. G. M. Sheldrick, *SHELXL97: Program for the Refinement of Crystal Structures from Diffraction Data* (University of Göttingen, Göttingen, Germany, 1997).
5. *International Tables for Crystallography, Vol. C: Mathematical, Physical, and Chemical Tables*, Ed. by E. Prince, 3rd ed. (Kluwer, Dordrecht, The Netherlands, 2004), Tables 4.2.6.8 and 6.1.14.
6. O. V. Yakubovich, I. M. Still, P. G. Gavrilenko, and V. S. Urusov, *Kristallografiya* **50** (2), 226 (2005) [*Crystallogr. Rep.* **50** (2), 194 (2005)].
7. O. Crottaz, F. Kubel, and H. Schmid, *J. Solid State Chem.* **120**, 60 (1995).
8. S. V. Krivovichev and C. Burns, *Mineral. Mag.* **64**, 1069 (2000).
9. G. Giuseppetti, F. Mazzi, and C. Tadini, *Neues Jahrb. Mineral., Monatsh.*, No. 6, 255 (1990).
10. I. M. Steele, J. J. Pluth, and A. Livingstone, *Mineral. Mag.* **62**, 451 (1998).
11. I. M. Steele, J. J. Pluth, and A. Livingstone, *Eur. J. Mineral.* **11**, 493 (1999).
12. H. I. Strunz and E. N. Nickel, *Strunz Mineralogical Tables* (E. Schweizerbart'sche, Stuttgart, Germany, 2001).
13. S. P. Saburov, S. N. Britvin, G. K. Bekenova, et al., *Am. Mineral.* **90**, 1163 (2005).
14. M. Uehara, A. Yamazaki, and S. Tsutsumi, *Am. Mineral.* **82**, 416 (1997).
15. A. R. Kampf, L. L. Jackson, G. B. Sidder, et al., *Am. Mineral.* **77**, 1107 (1992).
16. P. J. Dunn, R. S. W. Braithwaite, A. C. Roberts, and R. A. Ramik, *Am. Mineral.* **75**, 702 (1990).
17. M. J. Wilson, J. D. Russel, J. M. Tait, et al., *Mineral. Mag.* **48**, 127 (1984).
18. R. V. Gaines, P. B. Leavens, and J. A. Nelen, *Am. Mineral.* **64**, 355 (1979).
19. D. E. Appleman, H. T. Evans, G. L. Nord, et al., *Mineral. Mag.* **51**, 417 (1987).
20. S. Merlino, *Acta Crystallogr., Sect. B: Struct. Sci.* **28**, 2726 (1972).
21. W. Mikenda, F. Pertlik, P. Povondra, and J. Ulrych, *Mineral. Petrol.* **61**, 199 (1997).
22. N. V. Belov, *Essays on Structural Mineralogy* (Nedra, Moscow, 1976) [in Russian].
23. A. E. Lapshin, N. V. Borisova, V. M. Ushakov, and Yu. F. Shepelev, *Zh. Neorg. Khim.* **51** (3), 487 (2006) [*Russ. J. Inorg. Chem.* **51** (3), 438 (2006)].

Translated by O. Borovik-Romanova

SPELL: 1. exanining